BIOMOLECULES & THERAPEUTICS

Original Article
Biomol Ther 29(5), 551-561 (2021)

Platelet-Derived Growth Factor Receptor-α Subunit Targeting Suppresses Metastasis in Advanced Thyroid Cancer *In Vitro* and *In Vivo*

Ching-Ling Lin[1,2,3], Ming-Lin Tsai[4], Yu-hsin Chen[1,2,5], Wei-Ni Liu[6], Chun-Yu Lin[7,8], Kai-Wen Hsu[9,10], Chien-Yu Huang[11,12], Yu-Jia Chang[13,14], Po-Li Wei[11,14,15,16], Shu-Huey Chen[17,18], Li-Chi Huang[1,2,*] and Chia-Hwa Lee[6,14,19,*]

[1]Department of Internal Medicine, Cathay General Hospital, Taipei 10630,
[2]Department of Endocrinology and Metabolism, Cathay General Hospital, Taipei 10630,
[3]Department of Internal Medicine, School of Medicine, College of Medicine, Taipei Medical University, Taipei 11031,
[4]Department of General Surgery, Cathay General Hospital, Taipei 10630,
[5]Department of Cytology, Cathay General Hospital, Taipei 10630,
[6]School of Medical Laboratory Science and Biotechnology, College of Medical Science and Technology, Taipei Medical University, Taipei 11031,
[7]Institute of Bioinformatics and Systems Biology, National Yang Ming Chiao Tung University, Hsinchu 30010,
[8]Center for Intelligent Drug Systems and Smart Bio-Devices, National Yang Ming Chiao Tung University, Hsinchu 30010,
[9]Institute of New Drug Development, China Medical University, Taichung 40402,
[10]Research Center for Cancer Biology, China Medical University, Taichung 40402,
[11]Department of Surgery, School of Medicine, College of Medicine, Taipei Medical University, Taipei 11031,
[12]Division of General Surgery, Department of Surgery, Shuang Ho Hospital, Taipei Medical University, Taipei 11031,
[13]Graduate Institute of Clinical Medicine, College of Medicine, Taipei Medical University, Taipei 11031,
[14]TMU Research Center of Cancer Translational Medicine, Taipei Medical University, Taipei 11031,
[15]Division of Colorectal Surgery, Department of Surgery, Taipei Medical University Hospital, Taipei Medical University, Taipei 11031,
[16]Graduate Institute of Cancer Biology and Drug Discovery, Taipei Medical University, Taipei 11031,
[17]Department of Pediatrics, School of Medicine, College of Medicine, Taipei Medical University, Taipei 11031,
[18]Department of Pediatrics, Shuang Ho Hospital, Taipei Medical University, New Taipei City 23561,
[19]Ph. D. Program in Medical Biotechnology, College of Medical Science and Technology, Taipei Medical University, Taipei 11031, Taiwan

Abstract

Thyroid cancer is the most common endocrine malignancy. Patients with well-differentiated thyroid cancers, such as papillary and follicular cancers, have a favorable prognosis. However, poorly differentiated thyroid cancers, such as medullary, squamous and anaplastic advanced thyroid cancers, are very aggressive and insensitive to radioiodine treatment. Thus, novel therapies that attenuate metastasis are urgently needed. We found that both PDGFC and PDGFRA are predominantly expressed in thyroid cancers and that the survival rate is significantly lower in patients with high PDGFRA expression. This finding indicates the important role of PDGF/PDGFR signaling in thyroid cancer development. Next, we established a SW579 squamous thyroid cancer cell line with 95.6% PDGFRA gene insertion and deletions (indels) through CRISPR/Cas9. Protein and invasion analysis showed a dramatic loss in EMT marker expression and metastatic ability. Furthermore, xenograft tumors derived from PDGFRA gene-edited SW579 cells exhibited a minor decrease in tumor growth. However, distant lung metastasis was completely abolished upon PDGFRA gene editing, implying that PDGFRA could be an effective target to inhibit distant metastasis in advanced thyroid

Open Access **https://doi.org/10.4062/biomolther.2020.205**

Received Nov 12, 2020 **Revised** Apr 22, 2021 **Accepted** Apr 23, 2021
Published Online May 25, 2021

***Corresponding Authors**
E-mail: chlee@tmu.edu.tw (Lee CH), likih@seed.net.tw (Huang LC)
Tel: +886-2-27361661 (Lee CH), +886-2-27082121 (Huang LC)
Fax: +886-2-27395133 (Lee CH), +886-2-27016818 (Huang LC)

cancers. To translate this finding to the clinic, we used the most relevant multikinase inhibitor, imatinib, to inhibit PDGFRA signaling. The results showed that imatinib significantly suppressed cell growth, induced cell cycle arrest and cell death in SW579 cells. Our developed noninvasive apoptosis detection sensor (NIADS) indicated that imatinib induced cell apoptosis through caspase-3 activation. In conclusion, we believe that developing a specific and selective targeted therapy for PDGFRA would effectively suppress PDGFRA-mediated cancer aggressiveness in advanced thyroid cancers.

Key Words: Advanced thyroid cancer, PDGFRA, CRISPR/Cas9, Lung distant metastasis, Imatinib

INTRODUCTION

Platelet-derived growth factor (PDGF) is a proangiogenic factor that was isolated from human platelets (Clark *et al*., 1989; Brill *et al*., 2004). PDGFs are a variety of strong mesenchymal cell mitogenic agents and growth chemokines; they are also important modifiers for normal and pathological vascular development (Peterson *et al*., 2012; Corey *et al*., 2016). The latest findings show that PDGFs regulate tumor growth and metastasis by targeting malignant cells, vascular cells, and stromal cells (Chaudhry *et al*., 1992; Lindmark *et al*., 1993; Shao *et al*., 2000). To date, five PDGF ligands have been identified: PDGF-AA (PDGFA), PDGF-BB (PDGFB), PDGF-CC (PDGFC), PDGF-DD (PDGFD) and the PDGF-AB heterodimer (PDGFAB) (Chen *et al*., 2013). In cells, three different PDGFR isomers specifically interact with these PDGFs: PDGFR-$\alpha\alpha$ (PDGFR-α), PDGFR-$\beta\beta$ (PDGFR-β) and $\alpha\beta$ heterodimer (PDGFR-$\alpha\beta$). The different ligand isoforms have variable affinities to the receptor isoforms that cause cross reactivity; for example, PDGFR-β is favored by PDGFB or PDGFD activation, whereas PDGFRA is most activated by PDGFA or PDGFB and PDGFAB.

PDGFR overexpression has been widely found in several cancers, including ovarian, breast, pancreatic and liver cancers (Jechlinger *et al*., 2006; Matei *et al*., 2007; Chu *et al*., 2013). In prostate cancers, a high level of PDGFD seems to be involved in osteoclast differentiation and cancer-induced distant bone metastasis (Huang *et al*., 2012). Furthermore, PDGFR-β expression, which is predominant in prostate cancer tumor stroma and nonmalignant surrounding regions, has been associated with poor cancer patient survival (Hagglof *et al*., 2010). On the other hand, PDGFD also plays an important role in PDGFD-overexpressing breast triggers tumor aggressiveness, which has been mechanistically linked to the activation of Notch and NF-κB signaling (Ahmad *et al*., 2011). However, the association between PDGF/PDGFR signaling and thyroid cancer development remains unclear. Thus, understanding the carcinogenic role of PDGFs/PDGFRs in thyroid cancer would provide a potential clinical treatment for attenuating distant cancer metastasis and could extend survival time in advanced thyroid cancer patients, especially for those who suffer from medullary and anaplastic thyroid cancers, who have 5-year relative survival rates of only 39% and 4%, respectively.

Thyroid cancer is rare, but it is the most frequent endocrine malignancy, accounting for approximately 4% of all human malignancies (Hayat *et al*., 2007). The prognosis of thyroid cancer is generally favorable, especially in cases of well-differentiated thyroid cancers, such as papillary and follicular cancers, which have an average survival rate of 95% at 40 years. In clinical observations, localized and regional thyroid cancers have the highest patient survival rate among all cancer types (99.9%, 97.6%), but the five-year survival rates for metastatic thyroid cancer are significantly worse (54.7%) (Kunadharaju *et al*., 2015). Statistical analysis indicates that approximately 30% of well-differentiated thyroid cancers ultimately spread to the lymph nodes in the neck, and only 4% spread outside of the neck to other organs such as the lungs and bone. On the other hand, poorly differentiated anaplastic, squamous and medullary thyroid cancers are more severe and life threatening, especially aggressive anaplastic and squamous thyroid cancers, which often exhibit distant metastasis when disease is diagnosed, whereas medullary thyroid cancers are often found with local recurrence. Of advanced thyroid cancer types, primary squamous thyroid cancer has lymph node involvement in 59% and distant metastases in 26% of cases, which causes the median survival of squamous thyroid cancer patients to be less than 8 months. All these metastatic thyroid cancers, including both well-differentiated and poorly differentiated thyroid cancers, share one unique characteristic: they easily spread to distant organs and are not sensitive to radioiodine exposure (Beckham *et al*., 2018), resulting in a lack of effective treatments.

For advanced thyroid cancer patients for whom radioactive iodine is no longer working, targeted therapy is the only anticancer strategy in the clinic. Currently, the FDA-approved targeted drugs for thyroid cancers are the multikinase inhibitors lenvatinib and sorafenib for differentiated thyroid cancer treatment and vandetanib and cabozantinib for medullary thyroid cancer treatment. These drugs mainly act by blocking the formation of new blood vessels and by targeting proliferation-related oncogenic proteins in thyroid cancers. However, it is not yet clear whether these drugs improve thyroid cancer patient overall survival. On the other hand, there is still no targeted therapy available for human squamous and anaplastic thyroid cancer treatment. This critical issue inspires us to explore a new era of novel targeted therapy for preventing the distant metastasis of advanced thyroid cancers.

To provide an available and effective targeted therapy for advanced thyroid cancers, we investigated whether PDGF/PDGFR signaling plays critical roles during thyroid oncogenesis. Using a gene expression database, we are able to understand the importance of specific PDGF/PDGFR subunit expression in thyroid cancers. Through CRISPR/Cas9 gene editing, we can uncover the biofunctional effect of PDGF/PDGFR subunits in advanced thyroid cancers. To translate the findings into the clinic, a selective PDGFR inhibitor can be further used to monitor the anticancer effect and the potential suppression of cancer aggressiveness in advanced thyroid cancers. The ultimate aim of this study was to provide an effective cancer therapy to block PDGF/PDGFR-induced cancer invasion signaling, thereby improving the poor survival rate of advanced thyroid cancer patients.

MATERIALS AND METHODS

Cell culture

Human thyroid squamous cell carcinoma SW579 cell line was purchased by Bioresource Collection and Research Center (BCRC), Hsinchu, Taiwan. The cells were maintained in Dulbecco's Modified Eagle Medium: Nutrient Mixture F-12 (DMEM/F-12) (Gibco, CA, USA). The cells were cultured with 10% (v/v) fetal bovine serum (FBS, Biological Industries, Kibbutz Beit-Haemek, Israel), 100 units/mL penicillin and 100 mg/mL streptomycin and were incubated at 37°C with 5.0% CO_2. The medium was replaced every two days and when cells reached 80% confluence, they were passaged using 0.25% trypsin/EDTA (Gibco, CA, USA).

Gene expression datasets

Gene microarray dataset was collected from Cancer Cell Line Encyclopedia (CCLE, https://portals.broadinstitute.org/ccle/) (Barretina *et al*., 2012) and thyroid cancer patient survival dataset was collected from The Human Protein Atlas (https://www.proteinatlas.org/) (Uhlen *et al*., 2015). Both gene and protein expression datasets were further analyzed by PDGF/PDGFR subunit expressions.

Immunohistochemistry

Immunocytochemistry of PDGFRA protein expressions was stained by PDGFRA antibody (CAB018143) from Cell Signaling Technology (Danvers, MA, USA) on human Papillary (Patient ID. 3490) thyroid cancers and normal thyroid gland tissues (Patient ID. 1922) Antibody ID. The tissue array images were obtained from Human Protein Atlas.

MTT cell viability assay

SW579 cell viability was determined using the 3-(4,5-dimethylthiazol-2-yl)-2,5-diphenyltetrazolium (MTT), which is based on reduction of the yellow MTT to purple formazan by living cells (Lee *et al*., 2010). In 96-well plates, 8×10^4 cells were seeded in 100 μL of DMEM/F12 per well and were exposed to different concentrations of imatinib. After 24 or 48 h of treatment, the medium was changed to fresh medium containing 1 μg/mL of MTT. Two h later, 100 μL of DMSO was added in each well and the absorbance at 570 and 630 nM was determined. The percentage of cell viability was calculated using a formula [percentage viability=(average OD of sample/average OD of control)×100].

Protein extraction, western blotting, and antibodies

For western blot analysis, SW579 cells or xenograft were washed once with ice-cold PBS and lysed with radioimmunoprecipitation assay (RIPA) lysis buffer containing protease inhibitors. Fifty micrograms of protein from each sample was resolved by sodium dodecyl sulfate polyacrylamide gel electrophoresis (SDS-PAGE) and transferred to a nitrocellulose membrane. The anti-GAPDH (sc-32233), anti-p-ERK (sc-7383), anti-t-AKT (sc-1618), anti-P53(sc-126) antibodies were purchased from Santa Cruz Biotechnology (Santa Cruz, CA, USA). The anti-c-PARP (#9541), anti-Slug (#9585), anti-t-ERK (#4695), anti-Vimentin (#5741), anti-E-Cadherin (#3195), anti-N-Cadherin (#3116) and anti-PDGFRA (#3174) antibodies were purchased from Cell Signaling Technology. The anti-P21 (GTX629543) and anti-P27 (GTX100446) antibodies were purchased from GeneTex International Corporation (Hsinchu, Taiwan). The secondary anti-mouse and anti-rabbit antibodies were purchased from Santa Cruz Biotechnology. Most of the primary antibodies were used at a 1:1,000 dilution with overnight hybridization, followed by a one-h incubation with a 1:4,000 dilution of the secondary antibodies.

Plasmid construction and lentiviral production

Lentiviral particles were produced by transient transfection of Phoenix-ECO cells (CRL-3214) using TransIT®-LT1 Reagent (Mirus Bio LLC, Madison, WI, USA). Guide oligonucleotides were phosphorylated, annealed, and cloned into the BsmBI site of the lentiCRISPR v2 vector (Addgene, 52961, kindly provided by Feng Zhang), according to the Zhang laboratory protocol (Shalem *et al*., 2014) (F. Zhang lab, MIT, Cambridge, MA, USA). All the plasmid constructs were verified by sequencing. The lentiCRISPR construct or the pLJM1-EGFP plasmid (Addgene plasmid #19319, a gift from David Sabatini) was co-transfected with pMD2.G (Addgene plasmid #12259) and psPAX2 (Addgene plasmid #12260, both kindly provided by Didier Trono, EPFL, Lausanne, Switzerland). Lentiviral particles were collected at 36 and 72 h and then concentrated with a Lenti-X Concentrator® (Clontech, Mountain View, CA, USA). The lentivirus concentration for each gene was quantified by Q-PCR. Biohazards and restricted materials were used in this study in accordance with the "Safety Guidelines for Biosafety Level 1 to Level 3 Laboratory" (Bayot and Limaiem, 2021). The protocol was approved by the Institutional Biosafety Committee at Taipei Medical University, Taipei, Taiwan.

Design of on-target and off-target sgRNAs for *PDGFRA* gene

Custom sgRNAs for *PDGFR* gene were designed using the MIT CRISPR Design website (http://crispr.mit.edu/) with the sequence of *PDGFR* (NM_006206.6). This website provides both on-target sequences and off-target possibilities. We determined the highest scoring off-target sequences in the *PDGFR* protein-coding region *PDGFR* sgRNA_1 for potential off-target gene editing.

Sanger sequencing and gene editing efficiency assay

Genomic DNA was extracted, and the *PDGFRA* DNA region was PCR-amplified using the following primers: *PDGFRA* exon 2 forward ATTCTTTCATCTTTCAGGCGTCT and *PDGFRA* exon 2 reverse CTAACAACATTTCAATGCCAACATTAT; *PDGFRA* exon 3 forward GCATCCTATTCAGAGCGT and *PDGFRA* exon 3 reverse TGTAAATGTGCCTGCCTTCAA. Off-target sequences were PCR-amplified using the following primers: CDKAL1, forward ACAGTGAAACTTGTTGAAGAG and reverse ACA CACAGGTAAATACTAGATACTAAT. The PCR products were purified using a PCR Clean-up Purification Kit and sequenced by Sanger sequencing using the forward PCR primers. The editing efficiency of the sgRNAs and the potential induced mutations were assessed using TIDE software (https://tide.nki.nl/; Netherlands Cancer Institute, Amsterdam, Netherlands), which required only two Sanger sequencing runs from wild-type cells and mutated cells.

RNA-guided engineered nuclease-restriction fragment length polymorphism (RGEN-RFLP) assay

PCR products (approximately 100 ng per assay) of the *PDGFRA* exon 2 DNA region were amplified by sense primer: GC GGCCTCTAATACGACTCACTATAGGGTAAGACCAGG-

AACGCCGGATGTTTTAGAG and reverse primer: AAAAAAG-CACCGACTCGGTGCCACTTT-TTCAAGTT. The PCR were collected, purified and incubated for 30 min at 37°C with Cas9 protein (30 nM) and sgRNAs (30 nM) in 10 μL of NEB buffer 3. After cleavage, RNase A (2 μg) was added, and the reaction mixture was incubated for 15 min at 37°C to remove RNA. Next, proteinase K (2 μg) was added, and the reaction mixture was incubated for 15 min at 58°C to remove the Cas9 protein. The products were resolved on 2% agarose gels and visualized by ethidium bromide (EtBr) staining.

Animal experiments

Four-week-old severe combined immunodeficient (SCID female, 4 weeks old) female mice were purchased from the National Science Council Animal Center (Taipei, Taiwan) and housed in micro-isolator cages at the Laboratory Animal Center in the Taipei Medical University, with the approval number of IACUC107-014.

Sixteen mice were anesthetized with 2% isoflurane, and the mammary pads of each mouse were implanted with 5×10^6 SC (scramble) or *PDGFRA* sgRNA_1 virus transfected SW579 cells (n=8 per group). The mouse body weight and tumor volumes were measured every week in week 3 after xenograft implantation. The mice were scarified in week 10. The xenograft and lung tissues were collected and preserved in PBS. All surgeries were performed under isoflurane anesthesia and all efforts were made to minimize suffering. During the experiment, no stress or abnormal behaviors due to tumor bearing were observed in the mice. The health status of the animals was monitored once daily by a qualified veterinarian. Food and water were replaced every two days.

Immunofluorescent (IF) staining

To investigate lung metastasis in the animal model, IF staining assay were performed on poly-L-lysine-coated slides. The slides were incubated with FITC-labeled anti-Vimentin antibodies for two h at room temperature, washed twice with phosphate-buffered saline, and incubated with secondary antibodies for an additional one h in a moist chamber at room temperature. The slides were stained with Hoechst 33258 for nuclei location and examined with a Leica DMI3000 B Fluorescence Microscopy Imaging System (Leica Microsystems, Wetzlar, Germany). To enhance the colour contrast of Vimentin and nuclei location, The FITC signal was displayed with green colour, and nuclei location was displayed with red colour.

Non-invasive apoptosis detection sensor (NIADS) bioluminescence assay

SW579 cells were transfected with NIADS lentivirus and puromycin antibiotic selected for two days. The NIADS expressing SW579 cells were seeding in 96 cells and treated with DMSO, 1 and 10 μM imatinib for 24 h. D-luciferin (1.5 mg/mL in PBS) was added to each well and photon counts were collected by SpectraMax® iD3 Multi-Mode Microplate Reader (Molecular Devices inc, Silicon Valley, CA, USA) system soon after luciferin addition.

Statistical analysis

All data are expressed as the mean ± standard error, and the differences were analyzed by Student's t-test for pairwise samples. All statistical comparisons were performed using SigmaPlot graphing software (Systat Software, San Jose, CA, USA) and Statistical Package for the Social Sciences v.13 (SPSS, Chicago, IL, USA). A p-value<0.05 was considered statistically significant, and all statistical tests were two-sided.

RESULTS

Characteristics of PDGF/PDGFR subunit expression in thyroid cancers

To reveal the distribution of PDGF/PDGFR expression in all human cancers, we used the Cancer Cell Line Encyclopedia (CCLE) pancancer database to characterize the expression of four PDGFs and three PDGFRs among 1024 human cancers across 24 tumor types. After characterizing the gene expression of thyroid cancer tissues and other cancer tissue types, it was shown that both PDGFC and PDGFRA are predominantly and significantly overexpressed in thyroid cancers compared with other cancer types (Fig. 1A). The mean fluorescence intensity-$\log^2$ of PDGFC gene expression was 9.08 ± 0.715 in thyroid cancer versus 6.66 ± 0.084 in other cancer types (5.35-fold, p=0.005), whereas the mean fluorescence intensity of PDGFRA gene expression was 5.24 ± 0.64 in thyroid cancers versus 4.28 ± 0.024 in other cancers (1.94-fold difference, p=0.011). The overexpression of both PDGFC and PDGFRA indicates that the PDGF/PDGFR pathway might play a unique oncogenic role during thyroid cancer development. In the current cancer treatment, most small molecule-based anticancer drugs are designed to target the tyrosine kinase domain of growth factor receptors on the cell membrane, causing a growth signal blockade and cytotoxic effects on growth factor receptor-overexpressing cancer cells. However, antibody-, nanoparticle- or ligand-mediated targeting of anticancer therapeutics has just recently been explored in clinical trials (Allen, 2002). Therefore, to integrate this finding into clinical therapy, we chose to further investigate the role of PDGFRA in thyroid cancers. To reveal how PDGFRA is expressed in different types of thyroid cancer patients, we used the Human Protein Atlas database to illustrate PDGFRA expression in both normal thyroid gland and thyroid cancer tissues (Uhlen *et al*., 2015). In the tissue microarray, the papillary subtype of thyroid cancer exhibited strong PDGFRA expression (Fig. 1B), whereas normal thyroid gland tissue demonstrated low to mild PDGFRA expression (Fig. 1C). Furthermore, the Kaplan-Meier plot illustrated that high PDGFRA expression in thyroid cancer is related to a lower patient survival probability (approximately 78%, n=101, p=0.022) than low PDGFRA expression in thyroid cancer (approximately 92%, n=400) in 501 thyroid cancer patients (Fig. 1D). The evidence above indicates that PDGFRA has great potential to be used as a biomarker and drugable target for thyroid cancer therapy.

PDGFRA gene targeting through CRISPR/Cas9 genomic editing

CRISPR/Cas9 genomic editing has been widely used to understand biofunctional alterations after gene and translated protein loss. To investigate the oncogenic role of PDGFRA in advanced thyroid cancer, we examined the utility of CRISPR/Cas9 genome editing by targeting two custom-designed protospacers on the *PDGFRA* locus on chromosome 4 (q12) by lentivirus transfection. As shown in the *PDGFRA* genomic map (Fig. 2A), protospacer 1 targets the negative strand of exon 2 of the *PDGFRA* gene, whereas protospacer 2 targets the plus

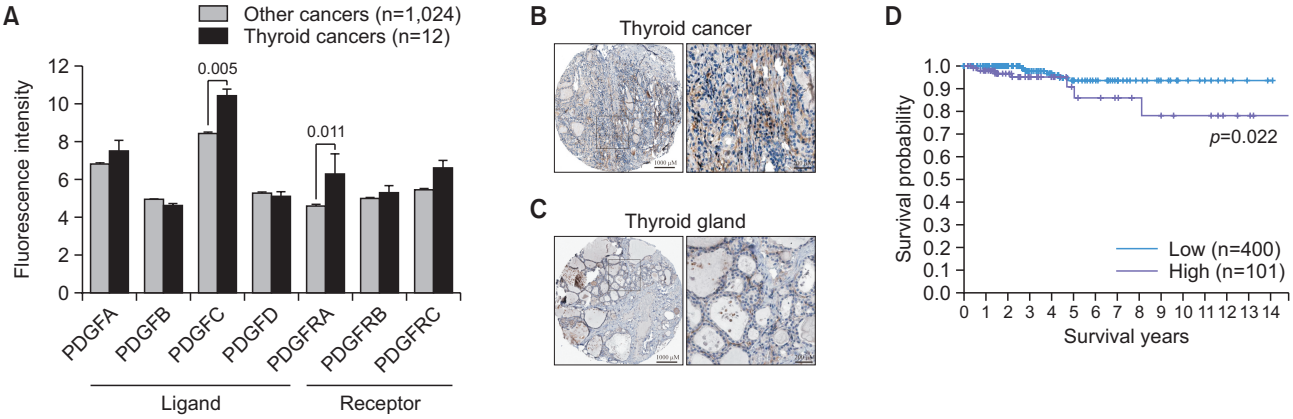

Fig. 1. Exploring PDGF/PDGFR subunit expression in human thyroid cancer cells. (A) Determination of PDGF/PDGFR subunit expression using the CCLE microarray gene database of all 1036 cancer cells. The samples were divided into thyroid tissue cancers (12 cells black bars) and other tissue cancers (1024 cancer cells, gray bars). The PDGF ligand includes PDGFA, PDGFB, PDGFC and PDGFD, whereas the PDGF receptor includes PDGFRA, PDGFRB and PDGFRC molecules. Data are presented as the mean and standard error of the fluorescence intensity from microarray analysis. Data were analyzed with Student's t-test; all *p*-values were two-sided. Immunocytochemistry of PDGFRA protein expression in (B) human papillary and (C) normal thyroid gland tissues was obtained from the Human Protein Atlas. The images are presented at low (left) and high microscope magnification (right). Scale bar=1000 and 200 μm, respectively. (D) Kaplan-Meier analysis of overall survival patients of a total of 501 clinical thyroid cancer patients showed that high *PDGFRA* expression (101 cases) predicted poor prognosis.

strand of exon 3 on the *PDGFRA* gene locus. According to our previous study (Huang *et al*., 2018), we knew that 90000-fold virus copy number input is the optimized virus transfection multiplicity of infection (MOI) in SW579 cells, and additional virus input is not able to enhance the transduction efficiency. After transduction with virus for three days, SW579 cells with the target scrambled (SC) lentivirus presented wild-type *PDGFRA* exon 2 and exon 3 sequences, as assessed by Sanger sequencing (Fig. 2B, 2C), showing no evidence of gene editing. However, transduction with the *PDGFRA* sgRNA_1 lentivirus carrying protospacer 1 (Fig. 2D) resulted in significant multiple-gene disruptions at the predicted cleavage sites (red arrowhead). On the other hand, transduction with the *PDGFRA* sgRNA_2 lentivirus carrying protospacer 2 (Fig. 2E) showed no evidence of gene editing at the predicted cleavage sites (red arrowhead), indicating that the *PDGFRA* sgRNA_1 lentivirus obtains a greater *PDGFRA* gene editing efficiency than the *PDGFRA* sgRNA_2 lentivirus. We next used TIDE gene editing software to analyze gene insertion and deletions (indels). The results not only showed that *PDGFRA* sgRNA_1 specifically targets the predicted cleavage sites (dotted line, Fig. 2F, 2G) but also illustrate that the *PDGFRA* sgRNA_1 virus has considerable gene editing efficiency, as 95.6% of the whole SW579 cell pool was edited (Fig. 2H). The most frequent gene editing indels in the *PDGFRA* sgRNA_1 cell pool were 1-bp deletions (41%) and other indels (28.9%). Furthermore, we performed RGEN-RFLP analysis to quantify the *PDGFRA* gene editing efficiency. The gel analysis of the gene editing efficiency showed that the SC sgRNA without Cas9 addition retained the full length of *PDGFRA* DNA (500 base pairs; uncut, Fig. 2I); however, the SC sgRNA with Cas9 addition fully cleaved DNA into 300- and 200-base-pair DNA fragments (cut, with an asterisk), indicating that the input sample is a 100% wild-type DNA sequence without any gene disruption. However, in the experimental sample, *PDGFRA* sgRNA_1-transfected SW579 cells with Cas9 addition retained 99% of the full-length DNA, indicating that the lentivirus-delivered *PDGFRA* sgRNA_1 obtained a great *PDGFRA* gene editing efficiency, causing the *PDGFRA* sgRNA_1 cannot target the *PDGFRA* DNA region and guide the Cas9 protein to execute DNA cleavage in SW579 advanced thyroid cancer cells.

PDGFRA gene editing inhibits aggressiveness and EMT marker expression in advanced thyroid cancers

Next, western blotting was used to reveal PDGFRA protein expression in *PDGFRA* sgRNA-introduced advanced thyroid cancer cells (Fig. 3A). Compared to wild-type SW579 cells, SW579 cells transfected with SC and PDGFRA sgRNA_2 showed complete loss of PDGFRA protein expression, whereas GAPDH internal control expression remained unchanged. To continue investigating whether the biological impact of cancer metastasis is affected by *PDGFRA* gene loss, we examined EMT marker expression and invasion ability in *PDGFRA* sgRNA_1-introduced advanced thyroid cancer cells (Fig. 3B). Western blotting showed that compared to parental SC cells, *PDGFRA* sgRNA_1-introduced SW579 cells had dramatically decreased protein expression of EMT markers, such as vimentin, N-cadherin and Slug, but increased expression of the epithelial marker E-cadherin. In addition, the microscopy images of the invasion assay illustrated that parental SC SW579 cells have a very strong cancer invasion ability (Fig. 3C, 3D). However, *PDGFRA* sgRNA_1-introduced SW579 cells completely lost their invasion ability, indicating that PDGFRA expression is a critical factor in manipulating cancer metastasis in advanced thyroid cancers. To clarify the potential off-target effect when using *PDGFRA* sgRNA_1 virus, we used the MIT CRISPR Design website to identify that the CDK5 regulatory subunit associated protein 1 like 1 (CDKAL1) gene is the most similar human genomic sequence to the *PDGFRA* sgRNA_1 sequence (Fig. 3E). We designed specific primers for the CDKAL1 gene, amplified the regions by PCR, and analyzed the DNA sequences by Sanger sequencing. The Sanger sequencing data clearly showed that neither SC nor *PDGFRA* sgRNA_1-introduced SW579 cells showed genomic editing of

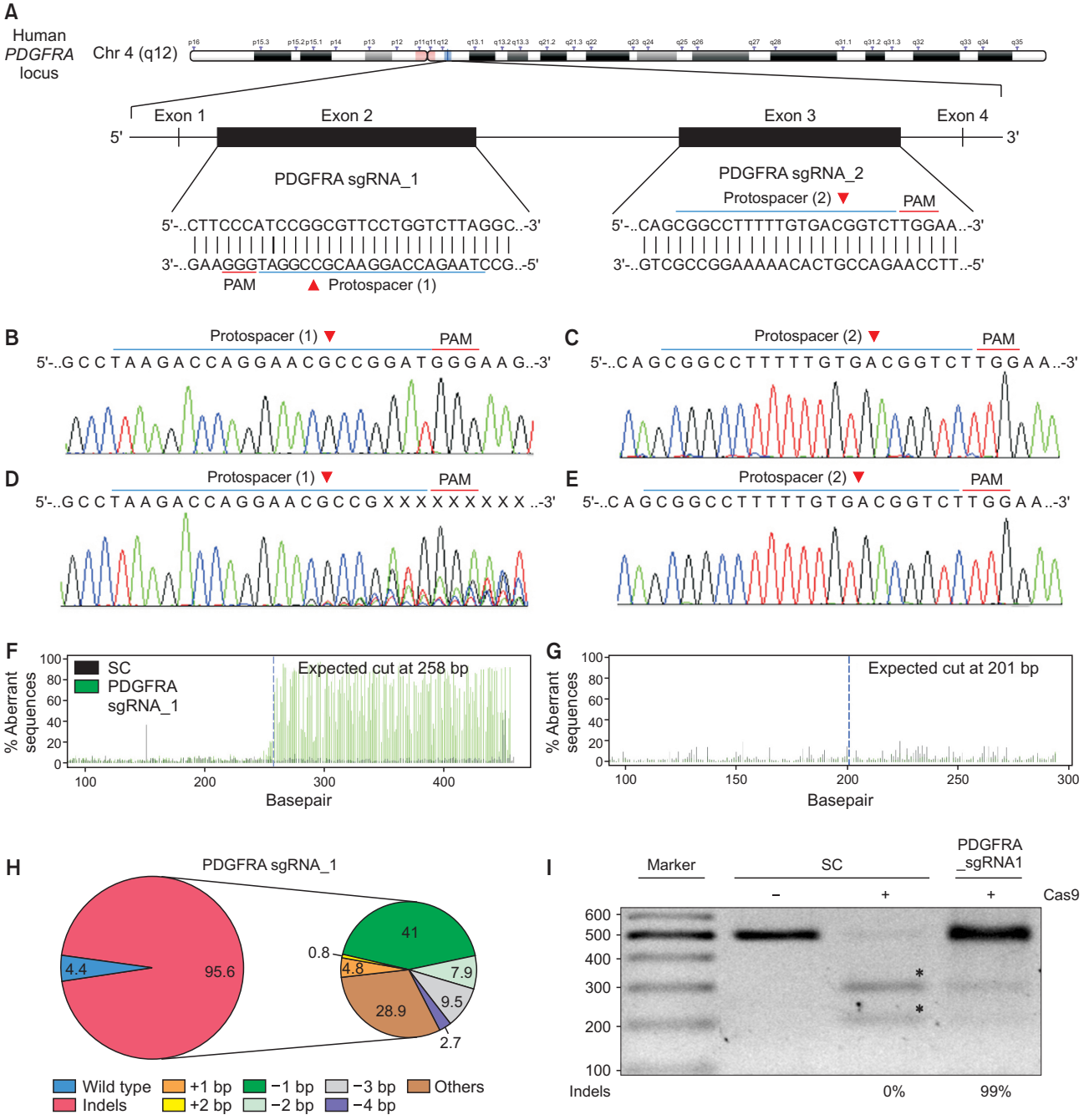

Fig. 2. CRISPR/Cas9-based *PDGFRA* gene editing in SW579 cells. (A) Schematic representation of the human *PDGFRA* DNA locus and two protospacer sequences (blue underline) of CRISPR/Cas9 gene editing. The protospacer adjacent motif (PAM, red underline) is the motif required for Cas9 nuclease activity. The arrowhead on the protospacer sequence indicates the expected cleavage site. Scrambled (SC) sgRNA and two *PDGFRA* sgRNAs containing lentivirus were independently delivered to SW579 cells. After transduction, DNA from virus-infected cells was purified and subjected to Sanger sequencing of *PDGFRA* exon 2 and exon 3. (B) and (C) show the wild-type *PDGFRA* sequences of SW579 cells. (D) *PDGFRA* sgRNA_1 produced a multiplex DNA sequence mixture around the expected Cas9 cleavage point in a pool of gene-edited cells, whereas (E) *PDGFRA* sgRNA_2 retained the wild-type DNA sequence. Using TIDE algorithm analysis, it was shown that (F) *PDGFRA* sgRNA_1 virus-transfected SW579 cells obtain an aberrant sequence signal in the scrambled mixture (green vs black), indicating that *PDGFRA* sgRNA_1 had a significantly high editing efficiency (indels, insertions and deletions) (G), whereas *PDGFRA* sgRNA_2 cells showed no indels presence in Sanger sequencing. (H) The pie chart demonstrates *PDGFRA* sgRNA_1 infection with different efficiency rates caused different gene indels in the whole cell population. The gene editing efficiency of *PDGFRA* sgRNA_1 was 95.6% (pink color), and the two most common -1 and other indels were presented at rates of 41% (green color) and 28.9% (brown color), respectively. (I) The *PDGFRA* gene in SW579 cells was further analyzed by RGEN-RFLP assay to quantify the gene editing efficiency. The agarose image of *PDGFRA* gene cleavage with specific *PDGFRA* sgRNA_1 and *PDGFRA* sgRNA_2 and Cas9 additions shows the indel percentage in the gene editing pool *in vitro*. The fragments of cleaved DNA are highlighted with an asterisk.

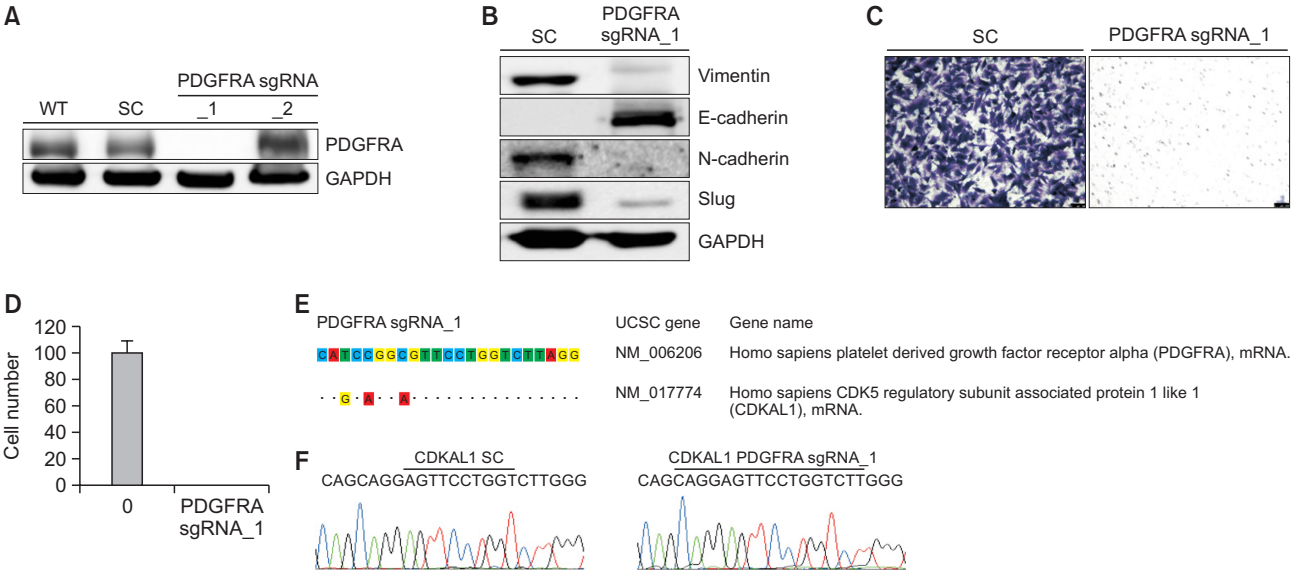

Fig. 3. The alteration of EMT markers and invasion ability in *PDGFRA* gene-edited cells. (A) Western blotting of PDGFRA protein expression in wild-type (WT), scrambled (SC), *PDGFRA* sgRNA_1 and *PDGFRA* sgRNA_2 virus-transfected SW579 cells. (B) Western blotting of EMT markers in SC- and *PDGFRA* sgRNA_1 virus-transfected SW579 cells. The EMT markers included vimentin, E-cadherin, N-cadherin and slug proteins, whereas GAPDH served as an internal loading control. (C) The Matrigel-based Transwell assay was used to assess the cancer invasion abilities of SC- and *PDGFRA* sgRNA_1 virus-transfected SW579 cells. Three days after plating, the cells that migrated through the Transwell membrane were washed, fixed and stained with 0.5% crystal violet. Images of migrated SC- and *PDGFRA* sgRNA_1 virus-transfected SW579 cells were taken at 100× microscope magnification and the cells were counted. Scale bar=100 μm. Data are presented as the mean and standard error of the number of invading cells from microarray analysis. Off-target investigation of the *PDGFRA*-targeted CRISPR/Cas9 system. (E) The CRISPR Design website was used to predict off-target candidate genes for *PDGFRA* sgRNA_1 viruses. Similarities from off-target candidate genes in the human DNA sequence are presented as dots, and mismatch sites are indicated by nucleotide substitution. (F) Sanger sequencing of SW579 cells infected with the SC or *PDGFRA* sgRNA_1 virus was used to determine the potential indel presence.

the CDKAL1 gene (Fig. 3F). This result proves the high specificity of the CRISPR/Cas9 system in targeting the *PDGFRA* gene and the potent anti-aggressiveness effects of PDGFRA targeted therapy on advanced thyroid cancer, indicating that this finding is worth translating into clinical therapy to prevent metastatic events in advanced thyroid cancer patients.

PDGFRA gene-edited SW579 cells lost aggressive cancer behaviors and EMT marker expression in spontaneous pulmonary metastasis xenograft models

To understand the impacts of *PDGFRA* gene editing on tumor progression and metastasis in advanced thyroid cancer cells *in vivo*, we subcutaneously implanted SC- and *PDGFRA* sgRNA_1-transfected SW579 cells into the mammary fat pad of SCID mice and allowed the xenografts to grow for 10 weeks. During this period, the body weights and tumor volumes were measured every week. In general, there was no significant change in body weight during the ten-week observation period (Fig. 4A). On the other hand, the xenografts of both the SC- and *PDGFRA* sgRNA_1-transfected SW579 groups exhibited similar tumor volumes during the whole observation period (Fig. 4B), whereas the xenografts in the *PDGFRA* sgRNA_1 groups exhibited decreased tumor growth rates after 8 weeks of implantation. This inhibition of tumor growth caused a minor decrease in tumor volume in the *PDGFRA* sgRNA_1 versus SC group (p=0.035), with volumes of 1,100 ± 94.9 mm^3 versus 1,820 ± 135.6 mm^3, respectively. Next, we determined whether *PDGFRA* sgRNA_1-transfected SW579 cancers could affect spontaneous pulmonary metastasis in an animal model. Lung tissues were collected from both SC and *PDGFRA* sgRNA_1-transfected SW579 mice and preserved in PBS. The tissues were sliced and stained with IF antibodies for vimentin (green) or with Hoechst stain (red) (Fig. 4C). Under fluorescent miscopy, the nodules of lungs from the SC group exhibited extremely high expression of vimentin protein, while the lungs from the *PDGFRA* sgRNA_1 group showed low and average levels of vimentin expression. There were also significantly more lung metastatic nodules (foci) in the SC group than in the *PDGFRA* sgRNA_1 group (p<0.01), with 12.4 ± 1.44 versus 0.8 ± 0.37 foci per lung tissue slide (Fig. 4D). Furthermore, using protein lysates from xenograft tumors, western blotting showed that compared to duplicate parental SC xenografts, duplicate *PDGFRA* sgRNA_1 gene-edited tumors had dramatically decreased protein expression of PDGFRA and EMT markers (Fig. 4E), such as vimentin, N-cadherin and Slug but increased expression of epithelial marker E-cadherin. The *in vitro* and spontaneous pulmonary metastasis animal model results suggest that targeting *PDGFRA* will be a convincing strategy for suppressing advanced thyroid tumorigenesis.

PDGFRA inhibitor enhances cancer cell apoptosis in SW579 cells

Several potent inhibitors of PDGFR kinases were identified in a previous study, including imatinib, linifanib, nintedanib and sorafenib (Kanaan and Strange, 2017). Among these po-

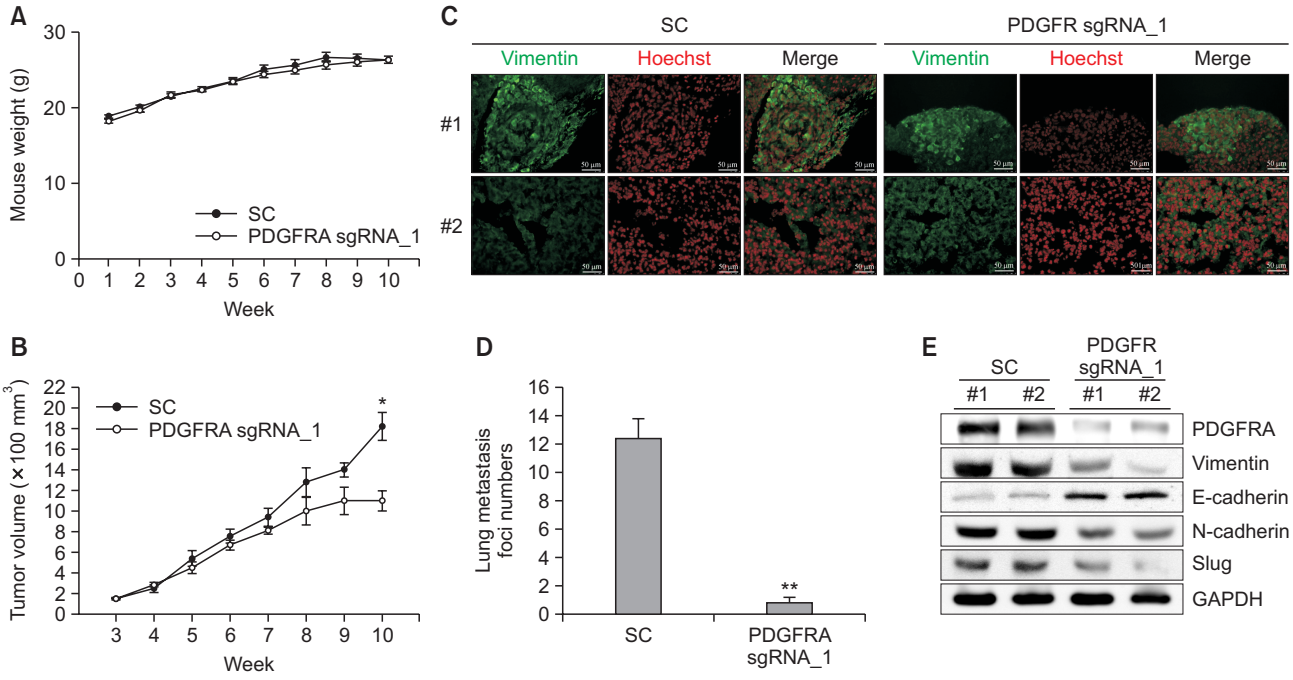

Fig. 4. *PDGFRA* gene editing decreased spontaneous pulmonary metastasis in an animal model. Female NOD-SCID mice were divided into 2 groups and SC- or *PDGFRA* sgRNA_1 virus-transfected SW579 cells were subcutaneously injected into the mammary fat pad. (A) Mouse body weights and (B) xenograft volumes were measured every week during tumor development. The mice were sacrificed 10 weeks after tumor implantation. (C) The lung tissue slides from the two groups were stained for IF with vimentin (green) or Hoechst (red). Scale bar=50 μm. (D) Spontaneous pulmonary metastatic foci were counted. The values are presented as the mean and standard error. Data were analyzed with Student's t-test; all *p*-values are two-sided. *p*-values less than 0.05 are indicated as *, whereas *p*-values less than 0.01 are indicated as **. (E) Xenografts from both the SC and *PDGFRA* sgRNA_1 groups were examined for PDGFRA and EMT marker expression. The EMT markers included vimentin, E-cadherin, N-cadherin and slug, and β-actin and GAPDH served as internal loading controls. The two randomly selected duplicate lung tissues and xenografts from each group are presented as #1 and #2 in the IF staining and protein analysis.

tential tyrosine kinase inhibitors (TKIs), imatinib is the most specific to PDGFR kinases, with half-maximal inhibitory concentrations (IC50s) of 71 nM against PDGFRA and 607 nM against PDGFRB kinase activity in lung cells (Medarametla *et al*., 2014). Imatinib is a common chemotherapeutic used to treat Ph-positive CML and ALL, certain types of gastrointestinal stromal tumors, systemic mastocytosis and myelodysplastic syndrome (Chen *et al*., 2020). Here, to investigate whether a PDGFRA inhibitor could potentially be used as an advanced thyroid cancer therapy, we tested the anticancer effects of imatinib on SW579 cells. We treated SW579 cells with different concentrations of imatinib (5-50 μM) for 24 and 48 h (Fig. 5A). The cell growth of MTT results revealed that imatinib had an IC50 of 16.7 μM in SW579 cells treated for 48 h, whereas imatinib had an IC50 of 21.9 μM in SW579 cells treated for 24 h, indicating that longer imatinib exposure has a better anti-cancer cell growth effect on SW579 cells, but the difference may not be significant. Next, we examined the signal transduction and cell cycle impacts of imatinib exposure. Western blotting showed that compared to the DMSO control, 1 μM and 10 μM imatinib treated SW579 cells significantly enhanced cell cycle arrest proteins, such as P21, P27 and P53 expressions (Fig. 5B). On the other hand, it is found imatinib treatment dramatically induced cell apoptosis signal, such as cleavage PARP expression, indicating imatinib would potentially be an alternative anti-advanced thyroid cancer therapy in clinic. Continue to investigate the cell growth impact of imatinib exposure, we found p-AKT and p-ERK expressions were significantly reduced under 1 μM and 10 μM imatinib treatments, compared to t-AKT, t-ERK and GAPDH loading controls (Fig. 5C, Supplementary Fig.). In triplicate experiments, it is found that under 1 μM and 10 μM imatinib treatments, p-AKT expression was decreased to 24.99% ± 1.68% and 18.79% ± 2.31% (Fig. 5D), whereas p-ERK expression was dropped to 62.99% ± 3.29% and 46.99% ± 4.24% (Fig. 5E), compare to DMSO control, respectively. To confirm the finding of imatinib-induced cell death in advanced thyroid cancers, we used a LIVE/DEAD assay to visualize imatinib-induced cancer cell apoptosis (Fig. 5F). The microscopy images show that SW579 cells underwent a great degree of cell death under 10 μM imatinib exposure than under DMSO control treatment, with 16.68 ± 4.16 versus 2.33 ± 0.58 dead cells per image (p=0.04, Fig. 5G). In our previous study, we established a bioluminescence-based live cell NIADS to evaluate the quantitative and kinetic analyses of apoptotic cell death (Hsu *et al*., 2018; Chen *et al*., 2019; Lin *et al*., 2019; Chen *et al*., 2020). Using this assay, we determined apoptotic events by simply measuring the bioluminescence activities of live cells. Here, we used the NIADS system to assess NIADS probe-expressing SW579 cells treated with DMSO, 1 and 10 μM imatinib for 24 h and then measured bioluminescence activity (Fig. 5H). The results showed a significantly increased number of apoptosis events in SW579 cells treated with 1 and 10 μM compared to those treated with DMSO. These results imply that imatinib inhibition of PDGFRA

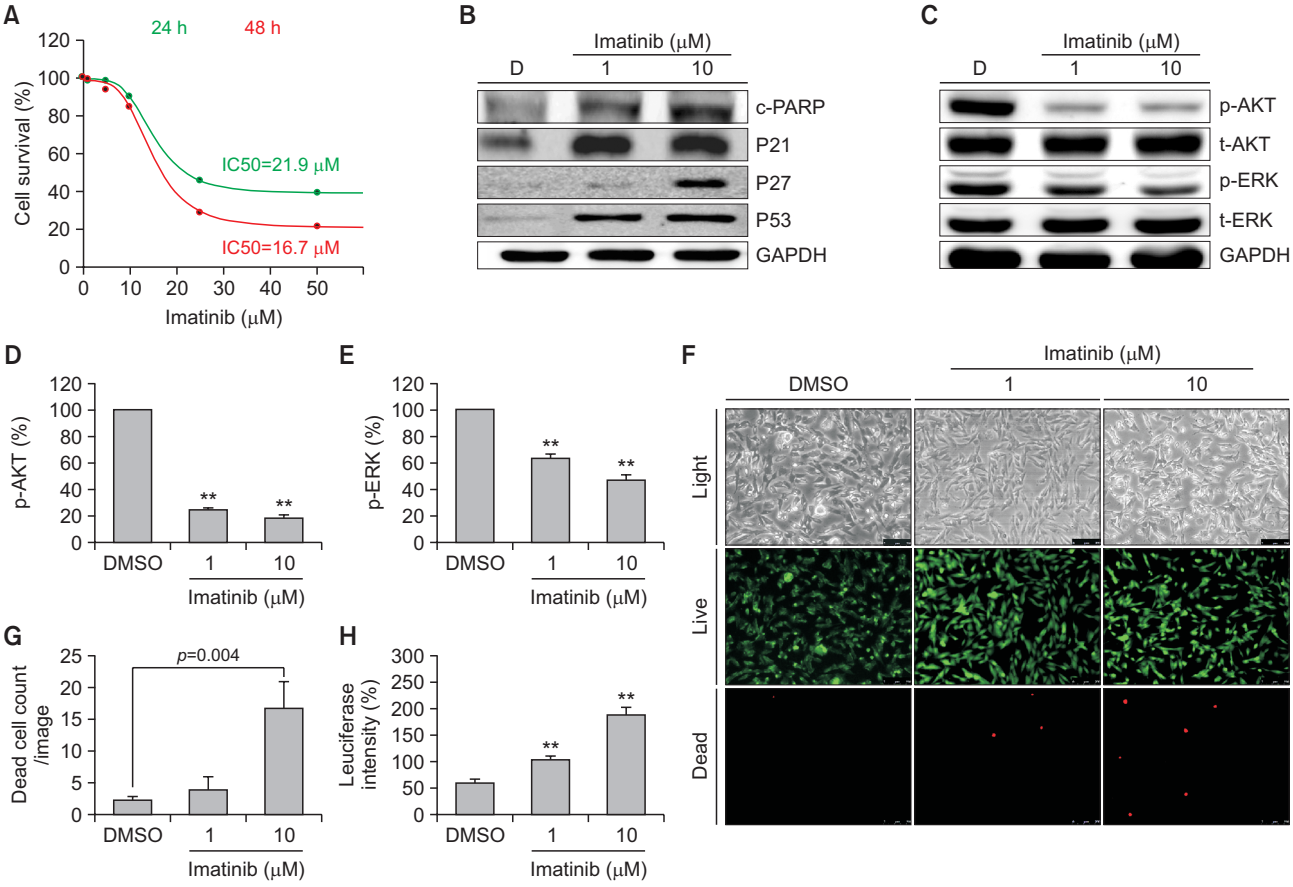

Fig. 5. Imatinib suppressed cell growth signals, induced cell cycle protein regulation and cell apoptosis in SW579 cells. (A) The IC50 values of DMSO control- or imatinib-treated SW579 cells were determined using MTT assays after treatment for 24 (green color) and 48 h (red color). Imatinib significantly (B) induced P21, P27, P53 and cleaved PARP (c-PARP) protein expressions and (C) inhibited AKR and ERK phosphorylations (p-AKT and p-ERK) in a dose-dependent manner, as indicated by western blot analysis. The (D) p-AKT and (E) p-ERK suppression ratios were measured in triplicate experiments and normalized by their total AKT (t-AKT) and ERK (t-ERK) protein expressions. The protein expression was qualified by ImageJ software. (F) The LIVE/DEAD cell viability assay was performed by DMSO control and 1 and 10 μM imatinib treatment of SW579 cells for 24 h. Cells were subjected to viability assays to identify live (green) and dead (red) cells. (G) Cell death was quantified by counting dead cells in a 50× microscope magnification image and analyzed for significance. Scale bar=250 μm. (H) The NIADS detected imatinib-induced cell apoptosis in SW579 cells. SW579 cells stably expressing the NIADS probe were exposed to either DMSO or 1 and 10 μM imatinib for 12 h, and luciferase activity was measured. The cells were exposed to luciferin at a concentration of 1.5 μg/mL before bioluminescence detection. The intense luciferase signal indicates apoptotic signals from the NIADS. The bar figure illustrates the percent mean and standard error of the photons in the treatment group compared to the DMSO group. Data were analyzed with Student's t-test; all *p*-values are two-sided. All p-values less than 0.01 are indicated as **.

activation significantly enhances cell cycle arrest and further induces cell apoptosis rather than decreasing cell growth.

DISCUSSION

Previous studies found that the ligand PDGFD was expressed at a higher level in tumor epithelium than in normal epithelium and that PDGFD plays a critical role in the epithelial-mesenchymal transition (EMT) of hepatoma cells (Wu *et al*., 2013). Other studies further discovered that PDGFD seems to be involved in the development of bone metastasis and is associated with increased Gleason and tumor stage (Sethi *et al*., 2010; Ustach *et al*., 2010). High PDGFD expression is also considered an independent prognostic factor in addition to histologic grade and tumor stage, and patients with high expression levels of PDGFD have a significantly poorer overall survival rate than patients with no expression (Ding *et al*., 2014). However, in the present study, we demonstrated that high expression of PDGFC and PDGFRA was found in thyroid cancers compared with other tissue cancers, whereas PDGFD was not significantly expressed in either thyroid cancers or other tissue cancers. This tissue-specific PDGF subunit expression result indicates that PDGFD may play a major role in regulating the distant metastasis of epithelial cells, whereas PDGFC/PDGFRA plays a similar aggressive role during thyroid cancer development.

Limited treatment options are available for patients with aggressive and radioiodine-refractory differentiated thyroid cancer. Conventional chemotherapy has limited efficacy and significant toxicities. The best efficacy chemotherapy drug for advanced thyroid cancer is doxorubicin, which remains the

most effective conventional agent (Sherman, 2010), but it still has poor response rates, with a partial response rate of 37% and a stable disease rate of 32% in metastatic differentiated thyroid cancer patients. However, doxorubicin seems to have better responses in patients with pulmonary metastases and a high performance status, with less response noted in bone or nodal metastases. Therefore, due to the limitation of monotherapy efficacy in differentiated thyroid cancer, the best strategies for metastatic thyroid cancer patients are likely combination regimens that include different anticancer agents.

Several researchers have investigated whether genetic mutations or polymorphisms in cancers should be taken into account when choosing high-efficacy treatment strategies. For example, the development of thyroid cancer was found to be associated with genetic alterations, such as BRAF mutation, *vascular endothelial growth factor* (*VEGF*) mutation (Lin and Chao, 2005), *KDR* (*VEGFR2*) mutation (Capp *et al*., 2010), *KIT/PDGFRA* mutation, and *PDGFRA* promoter polymorphisms (Agaimy *et al*., 2009; Kim *et al*., 2012). Among these mutations, the amino acid substitution at position 600 in *BRAF*, from a valine (V) residue to a glutamic acid (E) residue, denoted $BRAF^{V600E}$, is one the most important mutations in thyroid cancer (Xing, 2005) and is associated with the silencing of multiple thyroid-specific iodine-metabolizing genes (Liu *et al*., 2007; Tang and Lee, 2010). BRAF is a member of the RAF family of serine/threonine protein kinases and is suggested to be the most potent activator of MAP/ERK signaling. BRAF mediates the activation of RAS and the expression of transcription factors essential for cell growth, differentiation, proliferation, and survival. Accordingly, the $BRAF^{V600E}$ mutation occurs in approximately 45% of sporadic thyroid cancers, mostly in aggressive subtypes, such as tall-cell thyroid cancers (Kim *et al*., 2018). Notably, IGF-IR and PDGFR activation through AKT signaling is likely to be altered in feedback loops or through compensatory survival mechanisms when cancer cells are exposed to BRAF inhibitors (Villanueva *et al*., 2011). A combination targeted therapy approach using BRAF and PDGFR inhibitors seems to be a promising treatment for advanced thyroid cancer patients.

In summary, our study underscores the overriding contribution of PDGFRA in mediating cancer aggressiveness in advanced thyroid cancers. In the clinic, several potent PDGFR inhibitors, including multikinase inhibitors such as imatinib, sunitinib, sorafenib, pazopanib, and nilotinib, have been developed, and these therapies often obtain better results with combined use. In this study, we used the most specific PDGFRA FDA-approved anticancer drug, imatinib, for advanced thyroid cancer treatment. The results showed that cancer proliferation is inhibited by cell cycle protein regulation. Furthermore, the great invasion ability of advanced thyroid cancer was completely suppressed in PDGFRA gene-edited cells *in vitro* and in animal models, indicating that PDGFRA-based targeted therapy may be used to prevent the potential life-threatening event of thyroid cancer metastasis. Despite the strong evidence that PDGFRA regulates thyroid cancer metastasis in this study, no specific PDGFRA-targeting inhibitor has been approved by the FDA for anticancer purposes. Thus, how to further enhance the effectiveness and alleviate the side effects of combination therapy with selective PDGFR inhibitors in advanced thyroid cancer patients remains to be studied.

CONFLICT OF INTEREST

The authors declare no conflict of interest.

ACKNOWLEDGMENTS

We would like to acknowledge the following for their kind services: Facility Center of Taipei Medical University; Instrument Center and the Laboratory Animal Center at the National Defense Medical Center. This study was also partially supported by “TMU Research Center of Cancer Translational Medicine”, “the Center for Intelligent Drug Systems and Smart Bio-devices (IDS2B)” and “Drug Development Center, China Medical University” from The Featured Areas Research Center Program with in the frame work of the Higher Education Sprout Project by the Ministry of Education (MOE) in Taiwan. This study was supported by the Ministry of Science and Technology, grant Most-109-2628-B-038-014 for Dr. Lee, grant MOST-109-2314-B-281-007 for Dr. Lin, Cathay General Hospital, by the grant 108-CGH-TMU-04 for both Dr. Lin and Dr. Lee. This work was also financially supported from the Young Scholar Fellowship Program by the Ministry of Science and Technology (MOST) in Taiwan, Grant MOST 109-2636-B-009-007. None of the funding bodies were involved in the design of the study, the collection, analysis, and interpretation of the data, or the writing of the manuscript.

REFERENCES

Agaimy, A., Terracciano, L. M., Dirnhofer, S., Tornillo, L., Foerster, A., Hartmann, A. and Bihl, M. P. (2009) V600E BRAF mutations are alternative early molecular events in a subset of KIT/PDGFRA wild-type gastrointestinal stromal tumours. *J. Clin. Pathol.* **62**, 613-616.

Ahmad, A., Wang, Z., Kong, D., Ali, R., Ali, S., Banerjee, S. and Sarkar, F. H. (2011) Platelet-derived growth factor-D contributes to aggressiveness of breast cancer cells by up-regulating Notch and NF-kappaB signaling pathways. *Breast Cancer Res. Treat.* **126**, 15-25.

Allen, T. M. (2002) Ligand-targeted therapeutics in anticancer therapy. *Nat. Rev. Cancer* **2**, 750-763.

Barretina, J., Caponigro, G., Stransky, N., Venkatesan, K., Margolin, A. A., Kim, S., Wilson, C. J., Lehár, J., Kryukov, G. V., Sonkin, D., Reddy, A., Liu, M., Murray, L., Berger, M. F., Monahan, J. E., Morais, P., Meltzer, J., Korejwa, A., Jané-Valbuena, J., Mapa, F. A., Thibault, J., Bric-Furlong, E., Raman, P., Shipway, A., Engels, I. H., Cheng, J., Yu, G. K., Yu, J., Aspesi, P., Jr., de Silva, M., Jagtap, K., Jones, M. D., Wang, L., Hatton, C., Palescandolo, E., Gupta, S., Mahan, S., Sougnez, C., Onofrio, R. C., Liefeld, T., MacConaill, L., Winckler, W., Reich, M., Li, N., Mesirov, J. P., Gabriel, S. B., Getz, G., Ardlie, K., Chan, V., Myer, V. E., Weber, B. L., Porter, J., Warmuth, M., Finan, P., Harris, J. L., Meyerson, M., Golub, T. R., Morrissey, M. P., Sellers, W. R., Schlegel, R. and Garraway, L. A. (2012) The cancer cell line encyclopedia enables predictive modelling of anticancer drug sensitivity. *Nature* **483**, 603-607.

Bayot, M. L. and Limaiem, F. (2021) Biosafety guidelines. In Statpearls. Treasure Island (FL).

Beckham, T. H., Romesser, P. B., Groen, A. H., Sabol, C., Shaha, A. R., Sabra, M., Brinkman, T., Spielsinger, D., McBride, S., Tsai, C. J., Riaz, N., Tuttle, R. M., Fagin, J. A., Sherman, E. J., Wong, R. J. and Lee, N. Y. (2018) Intensity-modulated radiation therapy with or without concurrent chemotherapy in nonanaplastic thyroid cancer with unresectable or gross residual disease. *Thyroid* **28**, 1180-1189.

Brill, A., Elinav, H. and Varon, D. (2004) Differential role of platelet granular mediators in angiogenesis. *Cardiovasc. Res.* **63**, 226-235.

Capp, C., Wajner, S. M., Siqueira, D. R., Brasil, B. A., Meurer, L. and

Maia, A. L. (2010) Increased expression of vascular endothelial growth factor and its receptors, VEGFR-1 and VEGFR-2, in medullary thyroid carcinoma. *Thyroid* **20**, 863-871.

Chaudhry, A., Papanicolaou, V., Oberg, K., Heldin, C. H. and Funa, K. (1992) Expression of platelet-derived growth factor and its receptors in neuroendocrine tumors of the digestive system. *Cancer Res.* **52**, 1006-1012.

Chen, P. H., Chen, X. and He, X. (2013) Platelet-derived growth factors and their receptors: structural and functional perspectives. *Biochim. Biophys. Acta* **1834**, 2176-2186.

Chen, S. H., Chow, J. M., Hsieh, Y. Y., Lin, C. Y., Hsu, K. W., Hsieh, W. S., Chi, W. M., Shabangu, B. M. and Lee, C. H. (2019) HDAC1,2 knock-out and HDACi induced cell apoptosis in imatinib-resistant K562 cells. *Int. J. Mol. Sci.* **20**, 2271.

Chen, S. H., Hsieh, Y. Y., Tzeng, H. E., Lin, C. Y., Hsu, K. W., Chiang, Y. S., Lin, S. M., Su, M. J., Hsieh, W. S. and Lee, C. H. (2020) ABL genomic editing sufficiently abolishes oncogenesis of human chronic myeloid leukemia cells *in vitro* and *in vivo*. *Cancers (Basel)* **12**, 1399.

Chu, J. S., Ge, F. J., Zhang, B., Wang, Y., Silvestris, N., Liu, L. J., Zhao, C. H., Lin, L., Brunetti, A. E., Fu, Y. L., Wang, J., Paradiso, A. and Xu, J. M. (2013) Expression and prognostic value of VEGFR-2, PDGFR-beta, and c-Met in advanced hepatocellular carcinoma. *J. Exp. Clin. Cancer Res.* **32**, 16.

Clark, R. A., Folkvord, J. M., Hart, C. E., Murray, M. J. and McPherson, J. M. (1989) Platelet isoforms of platelet-derived growth factor stimulate fibroblasts to contract collagen matrices. *J. Clin. Invest.* **84**, 1036-1040.

Corey, D. M., Rinkevich, Y. and Weissman, I. L. (2016) Dynamic patterns of clonal evolution in tumor vasculature underlie alterations in lymphocyte-endothelial recognition to foster tumor immune escape. *Cancer Res.* **76**, 1348-1353.

Ding, J., Li, X. M., Liu, S. L., Zhang, Y. and Li, T. (2014) Overexpression of platelet-derived growth factor-D as a poor prognosticator in endometrial cancer. *Asian Pac. J. Cancer Prev.* **15**, 3741-3745.

Hagglof, C., Hammarsten, P., Josefsson, A., Stattin, P., Paulsson, J., Bergh, A. and Ostman, A. (2010) Stromal PDGFRbeta expression in prostate tumors and non-malignant prostate tissue predicts prostate cancer survival. *PLoS ONE* **5**, e10747.

Hayat, M. J., Howlader, N., Reichman, M. E. and Edwards, B. K. (2007) Cancer statistics, trends, and multiple primary cancer analyses from the Surveillance, Epidemiology, and End Results (SEER) Program. *Oncologist* **12**, 20-37.

Hsu, K. W., Huang, C. Y., Tam, K. W., Lin, C. Y., Huang, L. C., Lin, C. L., Hsieh, W. S., Chi, W. M., Chang, Y. J., Wei, P. L., Chen, S. T. and Lee, C. H. (2018) The application of non-invasive apoptosis detection sensor (NIADS) on histone deacetylation inhibitor (HDACi)-induced breast cancer cell death. *Int. J. Mol. Sci.* **19**, 452.

Huang, L. C., Tam, K. W., Liu, W. N., Lin, C. Y., Hsu, K. W., Hsieh, W. S., Chi, W. M., Lee, A. W., Yang, J. M., Lin, C. L. and Lee, C. H. (2018) CRISPR/Cas9 genome editing of epidermal growth factor receptor sufficiently abolished oncogenicity in anaplastic thyroid cancer. *Dis. Markers* **2018**, 3835783.

Huang, W., Fridman, Y., Bonfil, R. D., Ustach, C. V., Conley-LaComb, M. K., Wiesner, C., Saliganan, A., Cher, M. L. and Kim, H. R. (2012) A novel function for platelet-derived growth factor D: induction of osteoclastic differentiation for intraosseous tumor growth. *Oncogene* **31**, 4527-4535.

Jechlinger, M., Sommer, A., Moriggl, R., Seither, P., Kraut, N., Capodiecci, P., Donovan, M., Cordon-Cardo, C., Beug, H. and Grunert, S. (2006) Autocrine PDGFR signaling promotes mammary cancer metastasis. *J. Clin. Invest.* **116**, 1561-1570.

Kanaan, R. and Strange, C. (2017) Use of multitarget tyrosine kinase inhibitors to attenuate platelet-derived growth factor signalling in lung disease. *Eur. Respir. Rev.* **26**, 170061.

Kim, M. J., Kim, S. K., Park, H. J., Chung, D. H., Park, H. K., Lee, J. S., Kwon, K. H. and Chung, J. H. (2012) PDGFRA promoter polymorphisms are associated with the risk of papillary thyroid cancer. *Mol. Med. Rep.* **5**, 1267-1270.

Kim, W. W., Ha, T. K. and Bae, S. K. (2018) Clinical implications of the BRAF mutation in papillary thyroid carcinoma and chronic lymphocytic thyroiditis. *J. Otolaryngol. Head Neck Surg.* **47**, 4.

Kunadharaju, R., Goyal, G., Rudraraju, A. and Silberstein, P. T. (2015) New treatment options for metastatic thyroid cancer. *Fed. Pract.* **32**, 21S-26S.

Lee, C. H., Huang, C. S., Chen, C. S., Tu, S. H., Wang, Y. J., Chang, Y. J., Tam, K. W., Wei, P. L., Cheng, T. C., Chu, J. S., Chen, L. C., Wu, C. H. and Ho, Y. S. (2010) Overexpression and activation of the alpha9-nicotinic receptor during tumorigenesis in human breast epithelial cells. *J. Natl. Cancer Inst.* **102**, 1322-1335.

Lin, C. L., Tsai, M. L., Lin, C. Y., Hsu, K. W., Hsieh, W. S., Chi, W. M., Huang, L. C. and Lee, C. H. (2019) HDAC1 and HDAC2 double knockout triggers cell apoptosis in advanced thyroid cancer. *Int. J. Mol. Sci.* **20**, 454.

Lin, J. D. and Chao, T. C. (2005) Vascular endothelial growth factor in thyroid cancers. *Cancer Biother. Radiopharm.* **20**, 648-661.

Lindmark, G., Sundberg, C., Glimelius, B., Påhlman, L., Rubin, K. and Gerdin, B. (1993) Stromal expression of platelet-derived growth factor beta-receptor and platelet-derived growth factor b-chain in colorectal cancer. *Lab. Invest.* **69**, 682-689.

Liu, D., Hu, S., Hou, P., Jiang, D., Condouris, S. and Xing, M. (2007) Suppression of BRAF/MEK/MAP kinase pathway restores expression of iodide-metabolizing genes in thyroid cells expressing the V600E BRAF mutant. *Clin. Cancer Res.* **13**, 1341-1349.

Matei, D., Kelich, S., Cao, L., Menning, N., Emerson, R. E., Rao, J., Jeng, M. H. and Sledge, G. W. (2007) PDGF BB induces VEGF secretion in ovarian cancer. *Cancer Biol. Ther.* **6**, 1951-1959.

Medarametla, V., Festin, S., Sugarragchaa, C., Eng, A., Naqwi, A., Wiedmann, T. and Zisman, L. S. (2014) PK10453, a nonselective platelet-derived growth factor receptor inhibitor, prevents the progression of pulmonary arterial hypertension. *Pulm. Circ.* **4**, 82-102.

Peterson, J. E., Zurakowski, D., Italiano, J. E., Jr., Michel, L. V., Connors, S., Oenick, M., D'Amato, R. J., Klement, G. L. and Folkman, J. (2012) VEGF, PF4 and PDGF are elevated in platelets of colorectal cancer patients. *Angiogenesis* **15**, 265-273.

Sethi, S., Macoska, J., Chen, W. and Sarkar, F. H. (2010) Molecular signature of epithelial-mesenchymal transition (EMT) in human prostate cancer bone metastasis. *Am. J. Transl. Res.* **3**, 90-99.

Shalem, O., Sanjana, N. E., Hartenian, E., Shi, X., Scott, D. A., Mikkelsen, T. S., Heckl, D., Ebert, B. L., Root, D. E., Doench, J. G. and Zhang, F. (2014) Genome-scale CRISPR-Cas9 knockout screening in human cells. *Science* **343**, 84-87.

Shao, Z. M., Nguyen, M. and Barsky, S. H. (2000) Human breast carcinoma desmoplasia is PDGF initiated. *Oncogene* **19**, 4337-4345.

Sherman, S. I. (2010) Cytotoxic chemotherapy for differentiated thyroid carcinoma. *Clin. Oncol.* **22**, 464-468.

Tang, K. T. and Lee, C. H. (2010) BRAF mutation in papillary thyroid carcinoma: pathogenic role and clinical implications. *J. Chin. Med. Assoc.* **73**, 113-128.

Uhlen, M., Fagerberg, L., Hallstrom, B. M., Lindskog, C., Oksvold, P., Mardinoglu, A., Sivertsson, A., Kampf, C., Sjostedt, E., Asplund, A., Olsson, I., Edlund, K., Lundberg, E., Navani, S., Szigyarto, C. A., Odeberg, J., Djureinovic, D., Takanen, J. O., Hober, S., Alm, T., Edqvist, P. H., Berling, H., Tegel, H., Mulder, J., Rockberg, J., Nilsson, P., Schwenk, J. M., Hamsten, M., von Feilitzen, K., Forsberg, M., Persson, L., Johansson, F., Zwahlen, M., von Heijne, G., Nielsen, J. and Ponten, F. (2015) Proteomics. Tissue-based map of the human proteome. *Science* **347**, 1260419.

Ustach, C. V., Huang, W., Conley-LaComb, M. K., Lin, C. Y., Che, M., Abrams, J. and Kim, H. R. (2010) A novel signaling axis of matriptase/PDGF-D/ss-PDGFR in human prostate cancer. *Cancer Res.* **70**, 9631-9640.

Villanueva, J., Vultur, A. and Herlyn, M. (2011) Resistance to BRAF inhibitors: unraveling mechanisms and future treatment options. *Cancer Res.* **71**, 7137-7140.

Wu, Q., Wang, R., Yang, Q., Hou, X., Chen, S., Hou, Y., Chen, C., Yang, Y., Miele, L., Sarkar, F. H., Chen, Y. and Wang, Z. (2013) Chemoresistance to gemcitabine in hepatoma cells induces epithelial-mesenchymal transition and involves activation of PDGF-D pathway. *Oncotarget* **4**, 1999-2009.

Xing, M. (2005) BRAF mutation in thyroid cancer. *Endocr. Relat. Cancer* **12**, 245-262.